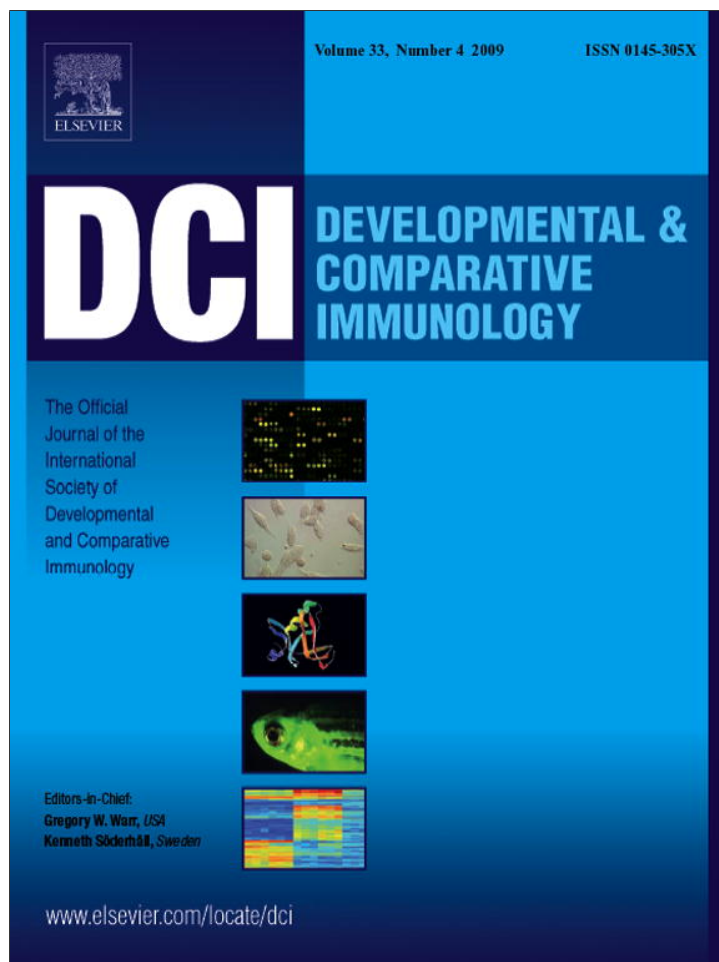


Provided for non-commercial research and education use.  
Not for reproduction, distribution or commercial use.



This article appeared in a journal published by Elsevier. The attached copy is furnished to the author for internal non-commercial research and education use, including for instruction at the authors institution and sharing with colleagues.

Other uses, including reproduction and distribution, or selling or licensing copies, or posting to personal, institutional or third party websites are prohibited.

In most cases authors are permitted to post their version of the article (e.g. in Word or Tex form) to their personal website or institutional repository. Authors requiring further information regarding Elsevier's archiving and manuscript policies are encouraged to visit:

<http://www.elsevier.com/copyright>



Contents lists available at ScienceDirect

## Developmental and Comparative Immunology

journal homepage: [www.elsevier.com/locate/dci](http://www.elsevier.com/locate/dci)

## Uncovering the evolutionary history of innate immunity: The simple metazoan *Hydra* uses epithelial cells for host defence

Thomas C.G. Bosch<sup>a,1,\*</sup>, René Augustin<sup>a,1</sup>, Friederike Anton-Erxleben<sup>a</sup>, Sebastian Fraune<sup>a</sup>, Georg Hemmrich<sup>a</sup>, Holger Zill<sup>a</sup>, Philip Rosenstiel<sup>b</sup>, Gunnar Jacobs<sup>b</sup>, Stefan Schreiber<sup>b</sup>, Matthias Leippe<sup>a</sup>, Mareike Stanisak<sup>a</sup>, Joachim Grötzinger<sup>c</sup>, Sascha Jung<sup>c</sup>, Rainer Podschun<sup>d</sup>, Joachim Bartels<sup>e</sup>, Jürgen Harder<sup>e</sup>, Jens-M. Schröder<sup>e</sup>

<sup>a</sup> Zoological Institute, Christian-Albrechts-University Kiel, Germany

<sup>b</sup> Institute of Clinical Molecular Biology, Christian-Albrechts-University Kiel, Germany

<sup>c</sup> Biochemical Institute, Christian-Albrechts-University Kiel, Germany

<sup>d</sup> Institute of Infection Medicine, Christian-Albrechts-University Kiel, Germany

<sup>e</sup> Clinical Research Unit, Department of Dermatology, Christian-Albrechts-University Kiel, Germany

## ARTICLE INFO

## Article history:

Received 15 September 2008

Received in revised form 10 October 2008

Accepted 13 October 2008

Available online 12 November 2008

## Keywords:

Innate immunity

Epithelial defence

Antimicrobial peptides

Toll-like receptors

*Hydra*

## ABSTRACT

Although many properties of the innate immune system are shared among multicellular animals, the evolutionary origin remains poorly understood. Here we characterize the innate immune system in *Hydra*, one of the simplest multicellular animals known. In the complete absence of both protective mechanical barriers and mobile phagocytes, *Hydra*'s epithelium is remarkably well equipped with potent antimicrobial peptides to prevent pathogen infection. Induction of antimicrobial peptide production is mediated by the interaction of a leucine-rich repeats (LRRs) domain containing protein with a TIR-domain containing protein lacking LRRs. Conventional Toll-like receptors (TLRs) are absent in the *Hydra* genome. Our findings support the hypothesis that the epithelium represents the ancient system of host defence.

© 2008 Elsevier Ltd. All rights reserved.

### 1. Introduction

To protect themselves against pathogens, vertebrates have developed a complex immune system that integrates fast innate defence mechanisms with delayed adaptive responses. Invertebrates rely exclusively on innate host defence systems to prevent infectious agents from entering the body [1]. Crucial elements of innate immunity include the Toll/Toll-like receptors, which detect conserved pathogen-associated molecular patterns (PAMPs) to initiate a complex antimicrobial response [2]. Although every multicellular organism and even single cells have effective defence mechanisms, the details of pathogen recognition, signalling mechanisms and antibacterial responses differ significantly among species indicating that ancient host defence has branched off into a

variety of unique and specialized systems during evolution [3]. Previous work on host defence strategies in invertebrates has largely focused on insects and nematodes [4–10]. Unlike these animals, Cnidaria are soft-bodied animals lacking mobile phagocytes, hemolymph and impermeable barriers, such as a cuticle or an exoskeleton, resulting in seemingly high vulnerability to pathogens [11]. To identify the evolutionary origin of genes involved in host defence, we recently scanned the EST and genomic resources in a number of cnidarian species and discovered unexpected complexity [12]. Here, we examine the nature of the defence strategies in *Hydra* (Fig. 1), which is a representative of this phylum and lives in freshwater habitats containing myriads of microbes. Scattered amidst the microbes are potential pathogens – bacteria, viruses, or protists – capable of tissue destruction and functional impairment. *Hydra* attaches to various substrata with foot epithelial cells and is in direct contact with the microflora which forms biofilm-communities (Fig. 1C). Bacteria in contact with *Hydra* include  $\gamma$ - and  $\beta$ -Proteobacteria [13]. When challenged by injury or tissue loss, *Hydra* is capable of extensive regeneration and, therefore, is a prime model to study evolutionary development and regeneration [14].

\* Corresponding author at: Zoological Institute, Christian-Albrechts University of Kiel, Am Botanischen Garten 1-9, 24118 Kiel, Germany. Tel.: +49 431 880 4169; fax: +49 431 880 4747.

E-mail address: [tbosch@zoologie.uni-kiel.de](mailto:tbosch@zoologie.uni-kiel.de) (Thomas C.G. Bosch).

<sup>1</sup> These authors contributed equally.

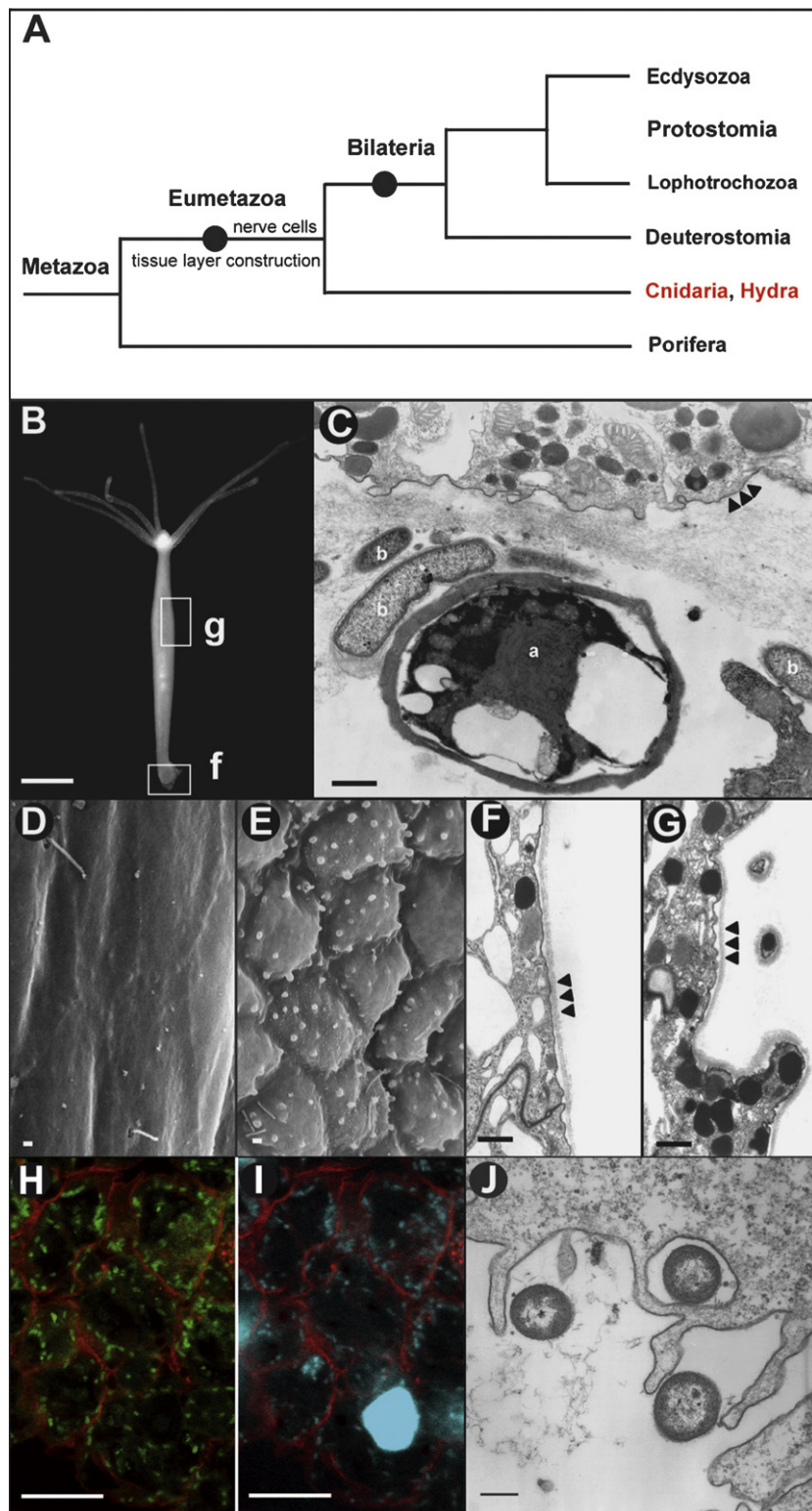


**Fig. 1.** *Hydra* and its cellular response to pathogen exposure. (A) Phylogenetic tree showing the basal position of Cnidaria as sister group to the Bilateria. (B) *Hydra magnipapillata*, g, gastric region examined by REM in (D–G), f, foot examined by TEM in (C). (C) TEM showing a foot epithelial cell in close contact with various microbes; a, alga; b, bacteria. Arrowheads indicate epithelial cell membrane. (D) REM showing the ectodermal epithelium in control polyps. (E) REM showing the ectodermal epithelium in polyps exposed to filtrates of adherent grown *Pseudomonas aeruginosa*. (F) TEM showing ectodermal epithelial cells in control polyps. Arrowheads indicate outer cell membrane and glycocalyx. Note the absence of any bacteria in the glycocalyx. (G) TEM showing ectodermal epithelial cells in *P. aeruginosa* filtrate-challenged polyps. Note the large number of intracellular granules. Arrowheads indicate outer cell membrane and glycocalyx. (H–J) Microscopic analysis of bacteria in endodermal epithelial cells. (H) CLSM showing GFP expressing bacteria engulfed during food uptake in endodermal epithelial cells. Red, phalloidin staining. (I) Cells shown in H stained with Hoechst. (J) Transmission electron micrograph of an endodermal epithelial cell engulfing bacteria.

Despite lacking many features of host defence of higher developed invertebrates, in *Hydra* both the ectodermal (Fig. 1D–G) as well as the endodermal epithelium (Fig. 1H–J) is remarkably well equipped to survive in an environment teeming with potential pathogens and to prevent infectious agents from entering the body. By using a combined biochemical, transcriptome and functional analysis approach we show that in the absence of mobile phagocytes, in *Hydra* effective innate immune responses are mediated by the epithelium and are based on unconventional TLR signalling. Our data indicate that the ancestral system of host defence is the inducible expression of antimicrobial peptides.

## 2. Materials and methods

### 2.1. Animals, nerve depletion, and immune challenge

We used *Hydra vulgaris* and two strains of *Hydra magnipapillata*. *H. magnipapillata* strain 105 is wildtype; strain sf-1 is a mutant strain containing a temperature-sensitive interstitial cell lineage [15]. Unless otherwise stated, animals were cultured using standard conditions at 18 °C. Polyps were exposed to *Pseudomonas aeruginosa* culture filtrate (generated from ATCC 33354, cultured at static conditions for 24 h in “MG”-medium, containing 40 mM K<sub>2</sub>HPO<sub>4</sub>, 30 mM glucose, 22 mM KH<sub>2</sub>PO<sub>4</sub>, 7 mM (NH<sub>4</sub>)<sub>2</sub>SO<sub>4</sub> and 0.5 mM MgSO<sub>4</sub>). Polyps were incubated in a 1:20 dilution of *P. aeruginosa* culture supernatant in *Hydra*-medium for 8–24 h. For control, polyps were incubated in a 1:20 dilution of MG medium in *Hydra* medium for the same period of time. WBB01 LPS from *Escherichia coli* (HL145) (gift from T. Gutschmann, research centre Borstel) was used to induce an immune response against gram-negative bacteria. Penta-/tetra-acyl from *E. coli* (GB1) LPS (inactive LPS) (gift from T. Gutschmann, Research Centre Borstel) was used as negative control. Both types of LPS were dispensed in 10 mM sodium phosphate buffer (pH 7) (stock concentration 100 µg/ml) vortexed, sonicated for 30 min, and subjected to several temperature cycles between 20 °C and 60 °C. Finally, the lipid suspensions were incubated at 4 °C for at least 12 h before use. Polyps were incubated with LPS at different concentrations (5–20 ng/ml) and for different times (15 min to 24 h). Nerve cells were eliminated as described previously [16] by culturing sf-1 animals for 25 days at 25 °C. Cell death was induced by incubating *Hydra magnipapillata* sf-1 polyps at 28 °C for 8 h [17]. Incubation experiments with flagellin were performed with *H. magnipapillata* polyps, which were kept in a 2.5 µg/ml flagellin solution for 0 h, 2 h and 4 h. Transfection with dsRNA was used to mimic the induction of immune response by viral infection. GFP [18] served as unrelated template for dsRNA production. DsRNA was produced with MEGAscript™ RNA Kit from Ambion according manuals instruction. 0.1 µg to 10 µg dsRNA was transferred into intact polyps by electroporation using previously established methods [19,20]. After 4 days of polyp recovery, total RNA was isolated using Trizol reagent (Invitrogen). Uric acid treatment was done as described [21] by incubating *H. vulgaris* polyps for 24 h in 20 µg/ml monosodium urate (MSU) (Sigma) or allopurinol (Sigma).

### 2.2. Antisera

The anti Periculin-1 polyclonal antiserum was raised in mouse against full-length recombinant Periculin-1 peptide in the Hybridoma Laboratory of Drs. V. Klimovich and M. Samoilovich (St. Petersburg). FITC conjugated anti-mouse Fab-fragments were used as secondary antibody.

### 2.3. Electron microscopy

For thin-section electron microscopy, polyps were fixed in 3.5% glutaraldehyde in 0.05 M cacodylate buffer, pH 7.4. After washing with 0.075 M cacodylate buffer for 30 min animals were post-fixed for 2 h with 1% OsO<sub>4</sub> in 0.075 M cacodylate buffer. After additional washing the tissue was dehydrated in ethanol and embedded in AGAR 100 resin/Agar Scientific Ltd. Ultrathin sections were contrasted with uranylacetate and lead citrate and analysed using a PHILIPS EM 208 S transmission electron microscope.

### 2.4. Antimicrobial activity

Antimicrobial activity of Hydramacin-1 was evaluated as described previously [22]. Briefly, test isolates were grown for 2–3 h in brain heart infusion broth at 36 ± 1 °C, washed three times in 10 mM sodium phosphate buffer (pH 7.4), supplemented with 1% tryptic soy broth (TSB), and adjusted to 10<sup>4</sup> to 10<sup>5</sup> bacteria/ml. A 100-µl volume of the bacterial suspension was mixed with 10 µl of Hydramacin-1 solution (range of final concentrations tested, 0.0125–100 µg/ml) and incubated at 36 ± 1 °C. After 2 h, CFU were determined. Bacterial suspensions supplemented with 10 µl of phosphate buffer/1% TSB instead of Hydramacin-1 served as negative controls. Results are given either as LD<sub>90s</sub> or as minimal bactericidal concentrations (MBCs) (≥99.9% killing). For assessing antimicrobial activity by the radial diffusion assay we measured growth inhibition of *E. coli* strain XL blue as described previously [16].

### 2.5. Molecular techniques

In situ hybridization and immunohistochemistry have been performed as described [23]. For functional analysis of *HyTRR-1*, *HyTRR-2* and *HyLRR-2*, we generated loss-of-function animals by dsRNA-mediated interference. dsRNA was synthesized using MEGAscript™ RNA Kit from Ambion. 10 µg of dsRNA was electroporated into intact polyps according to previously established protocols [19]. After 4 days of polyp recovery, total RNA was isolated using Trizol reagent from (Invitrogen). For RT-PCR, total RNA was isolated from immuno-challenged polyps using TRIzol reagent (Invitrogen). Aliquots of minimal 500 ng of total RNA were reverse transcribed as previously reported [19,23]. cDNA samples were equilibrated with primers against β-actin (18 cycles) and glyceraldehyde-3-phosphate dehydrogenase (GAPDH) (26 cycles) as described previously. In addition, a constitutively expressed endodermal epithelial cell specific gene (*arm-1*) (26 cycles) was used for equilibration. Water control and equilibration controls were included into every reaction. PCRs were performed according to standard profiles. Annealing temperatures were set due to *T<sub>m</sub>* of the specific primer pair. Only data obtained reproducibly in three to five independent experiments were further analyzed. Suppression subtractive hybridisation (SSH) [24] was performed to qualitatively compare the transcriptomes between immuno-stimulated and control tissue. For immuno-stimulation we used (i) *P. aeruginosa* culture filtrate-exposure and (ii) nerve depletion. Tester ds cDNA was obtained from polyps exposed for 8–24 h to *P. aeruginosa* supernatant. Driver ds cDNA was synthesized from untreated polyps. SSH was performed as described [23]. TIGR Indices Clustering Tools [25] were used for clustering the sequences. Data from the Hydra EST Project (approximately 175,000) and the sequence reads from the Hydra Genome project (approximately 6× coverage) were obtained from [www.hydrabase.org](http://www.hydrabase.org). Nucleotide, protein and translated BLAST engines at the NCBI server [26] were used for homology searches in public databases. Seqtools program (S.W. Rasmussen, [www.seqtools.dk](http://www.seqtools.dk)) was used for sequence analysis. ClustalW was used for sequence

alignments [27]. Version 3 of the MEGA software package [28] was used for phylogenetic tree construction. SMART [29], SignalP [30] and HMMer [31] were used for domain analysis.

## 2.6. HEK cell activation assay

All constructs were cloned into pcDNA3-Flag. All resulting proteins, therefore, have 3 Flag-tags at the N-terminus. HyLRR-2:HuTIR contains nucleotide 1–1455 of HyLRR-2 and nucleotide 1144–1710 of huIL1R1 mRNA, fused by PCR. HyLRR-2:HuTM + HuTIR contains nucleotide 1–1329 of HyLRR-2 and nucleotide 1009–1710 of huIL1R1 mRNA. HyTRR-1:HuTIR contains nucleotide 1–54 from HyLRR-2, nucleotide 1–815 of HyTRR-1 and nucleotide 1144–1710 of huIL1R1 mRNA. The whole open reading frame of HyLRR-2 was cloned into pcDNA3-Flag. Nucleotide counting starts with 1 at the ATG codon.

## 2.7. Transient transfection and NF- $\kappa$ B luciferase assay

Activation of transcription factor NF- $\kappa$ B was determined using a dual-luciferase reporter gene kit (Promega, Madison, WI) according to the manufacturer's manual. Cells seeded on 96-well plate were transfected with 12 ng/well of pNF- $\kappa$ B\_Luc plasmid (Stratagene, La Jolla, CA, USA) in combination with 3 ng/well of pRL-TK (Promega) and 35 ng/well expression plasmids. Empty vector (pcDNA3-Flag) was used as vector control. Cells were stimulated with the respective PAMPs for 12 h or left untreated. Cell lysates were analyzed on a Tecan Genios Pro microplate luminometer (Tecan Trading AG, Switzerland). All samples were measured in quadruplicates and all experiments were repeated independently at least three times. The results for NF- $\kappa$ B driven firefly luciferase activity were normalized using the reference plasmid and expressed as relative light units (RLU).

## 2.8. Genbank accession numbers

*Periculin-1* (AY649787); *Hydramacin-1* (DQ449931); *HyLRR-1* (DQ449927); *HyLRR-2* (DQ449928); *IL1R1* (NM\_000877), *HyTRR-1* (DQ449929); *HyTRR-2* (DQ449930); *MyD88* (CV182656); *IRAK* (DT608600); *TRAF* (gn|t|1004354542); *TAK1* (DN815379); *IKK* (CV985420).

## 2.9. Hydramacin-1 purification procedure

Hydramacin-1 was purified from *Hydra*-extracts with a similar strategy as used to purify human antimicrobial peptides from human stratum corneum [32]. Briefly, 10 g *H. vulgaris* was homogenized in 10 ml acidic ethanolic citrate buffer. After "diafiltration" (Amicon filters, cut off: 3 kDa) against 10 mM Tris-citrate buffer, pH 8.0, extracts were then applied to a heparin-sepharose cartridge (10 mm  $\times$  5 mm, Pharmacia, Freiburg, FRG), previously equilibrated with the diafiltration buffer. After washing, bound proteins were eluted with 2 ml of 2 M NaCl in 0.1 M Tris-citrate buffer and the heparin-bound material was then diafiltered against 0.1% (v/v) trifluoroacetic acid (TFA) in HPLC grade water. Heparin-bound material was purified by preparative wide-pore RP-8-HPLC using a column (300 mm  $\times$  7 mm, C8 Nucleosil, 250 mm  $\times$  12.6 mm, Macherey and Nagel) that was previously equilibrated with 0.1% (v/v) TFA in HPLC grade water containing 20% (v/v) acetonitrile. Proteins were eluted with a gradient of increasing concentrations of acetonitrile containing 0.1% (v/v) TFA (flow rate: 2 ml/min). Aliquots (10–30  $\mu$ l) of each fraction were lyophilized, dissolved in 5  $\mu$ l of 0.1% (v/v) aqueous acetic acid and tested for antimicrobial activity against *E. coli* ATCC 11303 by a radial diffusion plate

assay. Fractions containing strongest antimicrobial activity were further purified by MonoS<sup>®</sup> cation exchange HPLC followed by C2/C18-RP-HPLC as described for purification of HBD-3 [33] and RNase 7 [34]. Concentrations of proteins present in HPLC fractions were estimated via UV-absorbance integration at 215 nm or 280 nm using ubiquitin (Sigma, Munich) for calibration. Electrophoretic mobility was investigated using SDS-polyacrylamide gels (SDS-PAGE) in the presence of 8 M urea and tricine under non-reducing conditions as described for chemokines [35]. Peptides were visualized by silver staining [35]. Electrospray ionization mass spectrometry (ESI-MS)-analysis was performed in the positive ionization mode with a quadrupole-orthogonal-accelerating-time-of-flight-mass spectrometer (QTOF-II-hybrid-mass-spectrometer (Micromass, Manchester, UK). For mass spectrometric sequencing, proteins were reduced and alkylated, followed by trypsin-digestion. Tryptic fragments were further analysed by MS/MS-analysis and the data deconvoluted using MaxEnt3-software (Micromass).

## 2.10. Expression of recombinant Hydramacin-1

The bacterial expression vector pET-32a(+) encoding for a fusion protein consisting of thioredoxin, a histidine tag, an enterokinase cleavage site and the mature Hydramacin-1 was transformed into *E. coli* BL21 pLys. Liquid cultures were grown, and protein expression was induced by IPTG at an optical density (600 nm) of 0.5. After 4 h cells were harvested, lysed and the insoluble protein (inclusion bodies) fraction was isolated by centrifugation. The isolated inclusion bodies were washed and solubilized in 6 M guanidinium-hydrochloride, 50 mM Tris, pH 8.0 and purified with Ni-Agarose under denaturing conditions. The purified Hydramacin-1-fusion protein was then refolded by dialysis (50 mM Tris, pH 8.0) and proteolytically digested with enterokinase. Final purification was performed by cation-exchange chromatography followed by RP-HPLC (C18-column, Vydac) using a linear acetonitrile gradient.

## 3. Results

### 3.1. Bacterial pathogen-associated molecular patterns (PAMPs) cause drastic changes in *Hydra* epithelial cell morphology

Among the bacteria associated with *Hydra* are *Pseudomonas* species [13]. As shown in Fig. 1D–G, exposure of *H. magnipapillata* polyps to filtrates of adherent grown *P. aeruginosa* causes striking changes in ectodermal epithelial morphology. Ectodermal epithelial cells from stimulated polyps round up and form numerous blebs at the cell surface (Fig. 1E). Analysis of thin sections indicates that epithelial cells in *P. aeruginosa* filtrate-exposed *Hydra* polyps (Fig. 1G) contain a large number of granules. Thus, similar to immune cells in higher organisms [36], *Hydra* epithelial cells appear to respond to PAMPs by cytoskeletal rearrangement and increased secretory activity. In addition to ectodermal epithelial cells (Fig. 1D–G), the natural feeding behaviour of *Hydra* confronts also endodermal epithelial cells with large numbers of bacteria, illustrated by the uptake of GFP labelled bacteria (Fig. 1H–J), demanding effective endodermal epithelial defence mechanisms.

### 3.2. Identification of Hydramacin-1, an endermal *Hydra* peptide antibiotic

*Hydra* extracts contain strong microbicidal activity suggesting an innate antimicrobial barrier in *Hydra* epithelium. Since recently *Pseudomonas* species were detected in *Hydra* cultures [13], we

exposed *Hydra* polyps for 24 h to *P. aeruginosa* culture filtrate to identify constitutively as well as inducibly produced antimicrobial peptides (AMPs). *P. aeruginosa* culture filtrate is also known to be a potent innate immune inductor (JMS, pers. observation) containing LPS and flagellin. To isolate antimicrobial peptides, extracts of homogenized polyps were subjected to a heparin–sepharose affinity column. Bound peptides were further separated by preparative C8-reversed phase (RP)–HPLC. Using a radial diffusion antibacterial assay system, AMP-containing fractions were identified in many HPLC-fractions (data not shown). Fractions showing highest bactericidal activity were then further purified to homogeneity by cation-exchange-HPLC, followed by C2C18-RP-HPLC (Fig. S1). Electrospray ionisation-mass spectrometry (ESI-MS) analyses revealed a mass of 6994 Da for the principle AMP. By ESI-MS and MS/MS analyses we identified an eight amino acid peptide fragment (indicated by red letters in Fig. 2A) which mapped to a translated *Hydra* EST (CX833582). BLASTP searches revealed a significant match (Fig. 2B) to theromacin of *Aplysia californica*, an antibacterial peptide initially found in the leech *Theromyzon* [37]. This *Hydra* peptide, therefore, is referred to as Hydramacin-1. The *Hydramacin-1* cDNA contains a putative signal sequence directly followed by the mature peptide, encoding a basic cationic 60 aa peptide containing eight cysteines (Fig. 2A) with a calculated monoisotopic molecular mass of 7009 Da (for a four cysteine-bridges containing peptide). The 15 Da lower mass of the natural Hydramacin-1 indicates a posttranslational modification with a loss of one molecule NH<sub>3</sub> and addition of two hydrogens, suggesting that natural Hydramacin-1 contains a pyroglutamate at the N-terminus. In situ hybridization revealed that Hydramacin-1 mRNA is expressed exclusively in endodermal epithelium (Fig. 2C). To determine whether *Hydramacin-1* is constitutively expressed or inducible by microbial products, we exposed *Hydra* to ultrapure lipopolysaccharide (LPS) (WBBO1 LPS *E. coli* HL145) prior to RNA isolation. As shown in Fig. 2D, LPS upregulates *Hydramacin-1* expression in a dose-dependent manner at low concentrations indicating that *Hydramacin-1* is inducible by microbial products. Biologically inactive synthetic penta-/tetraacyl LPS (*E. coli* GB1) [38] served as a negative control.

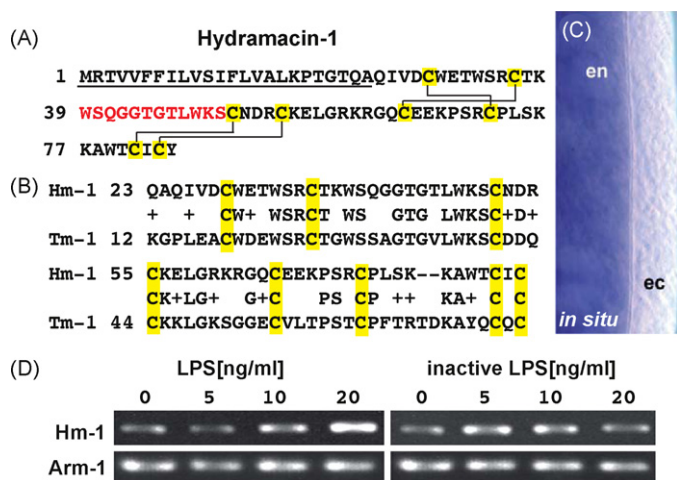


**Fig. 2.** Hydramacin-1, a host-defence genes in *Hydra*. (A) Hydramacin-1 amino acid sequence. Predicted structural features of Hydramacin-1 with a signal peptide (underlined) followed by a cationic region (pI value 9.1) with 8 cysteines (marked in yellow) that form four disulfide bridges (solid lines). Letters in red indicate amino acids determined by MS. (B) Alignment of Hydramacin-1 with theromacin of *Aplysia californica*; conserved cysteine residues are highlighted. (C) In situ hybridization shows that *Hydramacin-1* is expressed exclusively in the endoderm. (D) LPS induces the expression of *Hydramacin-1* (hm-1) in a dose-dependent manner.

**Table 1**  
Antimicrobial activity of Hydramacin-1.

Strain	MBC (μM)	LD <sub>90</sub> (μM)
<b>Gram negative</b>		
<i>C. freundii</i> UR 1776/03	0.9	0.2
<i>E. cloacae</i> ATTC 13047	1.8	0.4
<i>E. coli</i> ATTC 11775	0.9	0.4
<i>E. coli</i> ATTC 35218	0.4	0.2
<i>E. coli</i> D31	7.1	0.4
<i>K. pneumoniae</i> ATTC 13883	0.9	0.4
<i>P. aeruginosa</i> ATTC10145	>14.3	>14.3
<i>S. typhimurium</i> ATTC 13211	0.9	0.2
<i>Y. enterocolitica</i> NCTC 11174	0.4	0.2
<b>Multiresistant ESBL gram negative</b>		
<i>E. coli</i> ESBL Co 80	0.4	0.4
<i>E. coli</i> ESBL Co 82	0.4	0.2
<i>E. coli</i> ESBL Co 83	0.9	0.4
<i>E. coli</i> ESBL Co 84	0.9	0.2
<i>E. coli</i> ESBL Co 85	0.9	0.2
<i>K. oxytoca</i> ESBL 2	0.9	0.2
<i>K. oxytoca</i> ESBL 3	0.9	0.4
<i>K. oxytoca</i> ESBL 23	0.9	0.4
<i>K. oxytoca</i> ESBL 26	0.9	0.4
<i>K. pneumoniae</i> ESBL 8	3.6	0.9
<i>K. pneumoniae</i> ESBL 11	1.8	0.4
<i>K. pneumoniae</i> ESBL 20	0.9	0.4
<b>Gram positive</b>		
<i>B. megaterium</i> ATTC 14581	0.2	0.1
<i>E. faecalis</i> ATTC 29212	14.3	0.9
<i>S. aureus</i> ATTC 12600	>14.3	14.3
<i>S. epidermidis</i> ATTC 14990	>14.3	>14.3
<i>S. hominis</i> ATTC 27844	>14.3	3.6
<i>S. pneumoniae</i> ATTC 33400	>14.3	>14.3
<b>Fungi</b>		
<i>C. albicans</i> ATTC 10231	>14.3	>14.3
<i>C. albicans</i> ATTC 24433	>14.3	>14.3
<i>C. glabrata</i> ATTC 90030	>14.3	>14.3

### 3.3. Hydramacin-1 has high activity against numerous bacteria including antibiotic resistant human pathogens

To assess the antimicrobial activity of Hydramacin-1, we generated recombinant peptide from a fusion protein in *E. coli*. ESI-MS analyses revealed a mass of rHydramacin-1 of 6994 Da—identical with that of natural Hydramacin-1 and also containing a pyroglutamate at the N-terminus. When used in liquid growth inhibition assays against *Bacillus megaterium* ATCC14581 and *E. coli* D31, recombinant Hydramacin-1 showed a strong inhibitory effect on the growth of *B. megaterium* (data not shown). To study the antimicrobial activity of Hydramacin-1 against a variety of bacteria in more detail, we assessed the minimal bactericidal concentration (MBC) of Hydramacin-1. The results (Table 1) confirmed that Hydramacin-1 is highly active against *B. megaterium*. In addition, Hydramacin-1 was capable of killing a large number of human gram negative pathogens, including *E. coli*, *Klebsiella oxytoca* and *Klebsiella pneumoniae* strains which are resistant to all currently available antibiotics (Table 1), making Hydramacin-1 an interesting leading-structure for design of a novel generation of antibiotics. Although being able to kill *B. megaterium* at very low doses, Hydramacin-1 is not active against gram positive *Coccus* species. Hydramacin is also not active against gram negative non-fermentation species, and against *Candida albicans* (Table 1). The inability of Hydramacin-1 to kill or inhibit *P. aeruginosa* (Table 1) was surprising in light of the fact that (i) *Hydra* tissue has activity against *P. aeruginosa* (RA and TCGB, pers. observation) and (ii) that the supernatant used to induce the immune response was from *P. aeruginosa*. However, as described above, the supernatant also contains LPS, and LPS is a strong inductor of Hydramacin-1 (see

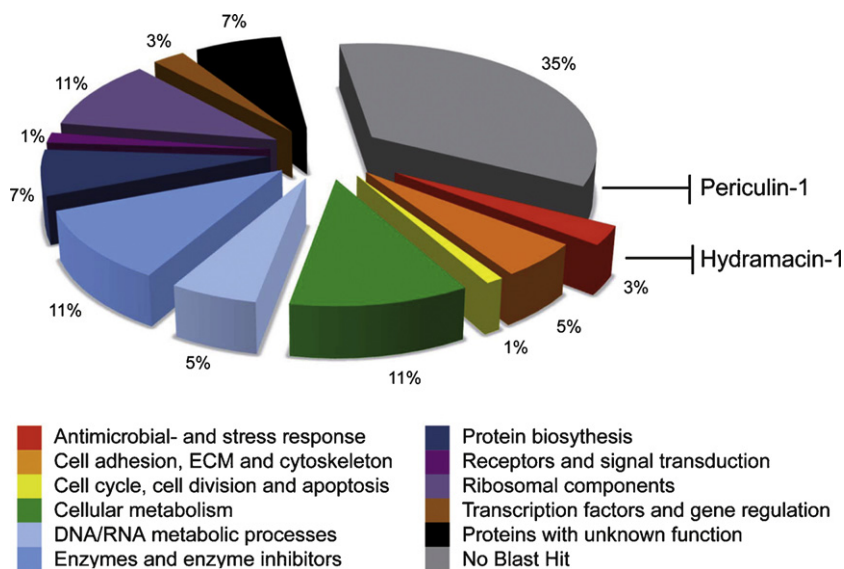


Fig. 3. Distribution of the *Hydra magnipapillata* SSH clusters and singletons annotated according to common Gene Ontology terms.

Fig. 2D). Thus, purification of Hydramacin-1 from an extract which was initially exposed to *P. aeruginosa* supernatant (see Fig. S1) and which in retrospect is expected to be able to induce Hydramacin-1 can be explained by the heterogeneity of the supernatant. The activity of the tissue extract against *Pseudomonas* most likely is due to the activity of not yet identified AMPs. While active against *E. coli* strains ATCC11775 and ATCC35218, Hydramacin-1 has a strongly reduced activity against *E. coli* strain D31 (Table 1), which is known for its reduced LPS structures in the outer cell membrane. This and the capacity of Hydramacin-1 to kill both gram positive and gram negative species may indicate a novel, not yet understood way of interaction of Hydramacin-1 with the bacterial membrane.

### 3.4. Identification of Periculin-1 as novel bactericidal *Hydra* peptide

To identify additional genes involved in innate immunity of *Hydra* and to produce cDNA libraries enriched for genes with functions in the immune response, we used suppression subtraction hybridisation (SSH). Since we have previously observed that nerve-depleted polyps show enhanced antimicrobial activity [16]. cDNA was prepared from polyps challenged with adherent *P. aeruginosa* culture supernatants and from nerve depleted polyps (see Section 2 for detail). 4894 sequences were obtained which could be grouped into 332 contigs and 95 singletons. As indicated in Fig. 3, 65% of the sequences showed BLAST matches to previously identified proteins and, therefore, could be functionally annotated according to common Gene Ontology (GO) terms [39]. The remaining 35% of protein encoding sequences showed no matches in any databank and, therefore, might represent novel genes. Among the known genes upregulated in immune-challenged polyps and annotated in the category “antimicrobial and stress response” was Hydramacin-1. The fact that both, the transcriptome analysis and the biochemical approach described above resulted in the isolation of Hydramacin-1 underlines the view that this peptide has a distinct function in host defence.

Among the 35% novel genes upregulated by *P. aeruginosa* filtrates (Fig. 3) we discovered the gene *Periculin-1*, termed due to its rapid response to a wide variety of bacterial and tissue “danger” signals (see below). Analysis of the deduced amino acid sequence of *Periculin-1* and the charge distribution within the molecule

reveals an anionic N-terminal region and an 8 cysteine residues containing cationic C-terminal region (Fig. 4A). No identifiable orthologues were found in any database. *Periculin-1* is expressed in the endodermal epithelium as well as in some interstitial cells in the ectoderm (Fig. 4B and D). To localize the *Periculin-1* peptide in *Hydra* tissue, a polyclonal anti-*Periculin-1* antiserum was raised in mice. We detected immunoreactive *Periculin-1* peptide in endodermal epithelial cells as well as in a subpopulation of ectodermal interstitial cells (Fig. 4E), at similar locations as *Periculin-1* mRNA. To assess the antimicrobial activity of *Periculin-1*, we generated recombinant peptide representing the cationic C-terminal region (Fig. 4A) in *E. coli*. When used against *B. megaterium* ATCC14581, we observed a bactericidal activity ( $LD_{90}$ ) of 0.2–0.4  $\mu$ M indicating that this peptide also is involved in the *Hydra* host defence.

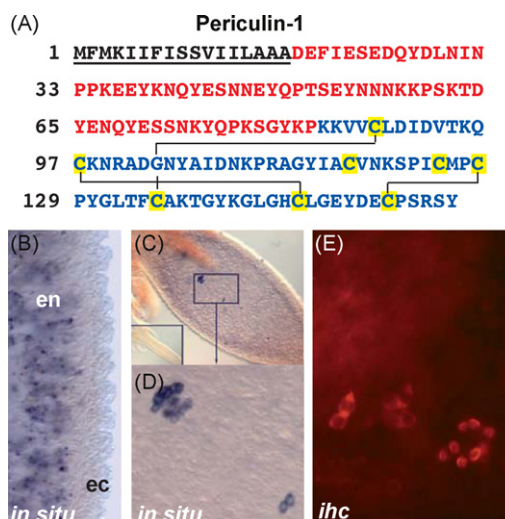
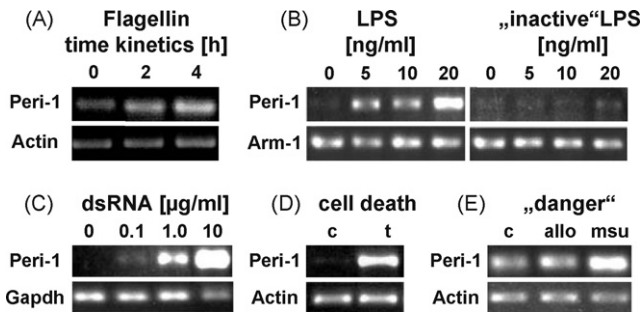


Fig. 4. *Periculin-1*, a novel host defence effector molecule in *Hydra*. (A) *Periculin-1* amino acid sequence and structural features. A signal peptide (underlined) is followed by an anionic (red amino acid residues; pI value 4.5) and a cationic (blue amino acid residues, pI value 8.7) domain which contains 8 cysteines (marked in yellow) predicting three disulfide bridges (solid lines). (B–D) *Periculin-1* mRNA is expressed in endodermal cells (B) as well as in interstitial cells in the ectoderm (C) and (D). (E) Polyclonal antiserum shows the *Periculin-1* peptide localized in the endoderm as well as in some ectodermal interstitial cells.



**Fig. 5.** *Periculin-1* expression is induced by a number of PAMPs. (A) Time kinetics of induction of expression of *Periculin-1* (Peri-1) by flagellin, actin, cDNA equilibration. (B) LPS induces expression of *Periculin-1* in a dose-dependent manner, Arm-1, cDNA equilibration. (C) dsRNA induces the expression of *Periculin-1*, Gapdh, cDNA equilibration. (D) Induction of *Periculin-1* mRNA-expression by signals from dying cells. c, control tissue; t, tissue which contains apoptotic cells (see Section 2 for details), actin, cDNA equilibration. (E) Induction of *Periculin-1* expression by danger signal monosodium urate (MSU). Allopurinol was used as control as described [21], actin, cDNA equilibration.

### 3.5. Microbial PAMP, flagellin, and endogenous “danger” signals upregulate the expression of *Periculin-1*

Most abundant bacteria species in *Hydra* are flagellated bacteria [13]. We, therefore, next examined whether bacterial flagellin can induce *Periculin-1* expression. As shown in Fig. 5A, exposure of *Hydra* to 2.5 µg/ml flagellin upregulates *Periculin-1* expression in a time dependent manner. Since *P. aeruginosa*-filtrates contain not only flagellin but also LPS, we also exposed *Hydra* to ultrapure LPS (WBB01 LPS *E. coli* HL145) [38] to analyze whether in addition to flagellin also LPS can induce *Periculin-1* expression. As shown in Fig. 5B, in addition to flagellin also LPS upregulates *Periculin-1* expression in a concentration dependent manner, whereas inactive synthetic penta-/tetraacyl LPS (*E. coli* GB1) [38] failed to induce *Periculin-1*.

Unexpectedly, introduction of dsRNA of unrelated sequence into *Hydra* polyps by electroporation (see Section 2) also caused a strong upregulation of *Periculin-1* expression in a dosage-dependent manner (Fig. 5C). Since double-stranded RNA is a viral replication intermediate and a potent stimulus to trigger host responses [40], the strong response of *Periculin-1* to the presence of “foreign” RNA may reflect an antiviral response. In contrast to *Periculin-1*, *Hydracinin-1* expression was not affected by dsRNA (data not shown).

Cell death plays an important role in *Hydra* tissue homeostasis [17,41,42] and may also be responsible for removal of infected cells. We, therefore, asked whether signals released by damaged or dying cells can also affect *Periculin-1* expression. Cell death was induced in *Hydra* mutant strain (*sf-1*) by temperature shock as described [17]. A high level of *Periculin-1* expression accompanies cell death signals in *Hydra* (Fig. 5D).

In vertebrates, one of the principal endogenous immunological “danger signals” released from injured or dying cells is monosodium urate (MSU), the end product of purine catabolism [21,43,44]. To investigate whether MSU can trigger *Periculin-1* expression, *Hydra* polyps were exposed to MSU for 24 h. As a negative control, polyps were treated with allopurinol, a structurally related but inactive molecule [21]. As shown in Fig. 5E, expression of *Periculin-1* is strongly upregulated after stimulation with MSU while allopurinol failed to induce *Periculin-1* transcription. Thus, uric acid appears to be a highly conserved endogenous danger signal. Taken together, the results indicate that a wide variety of bacterial and tissue components affect the expression of *Periculin-1*.

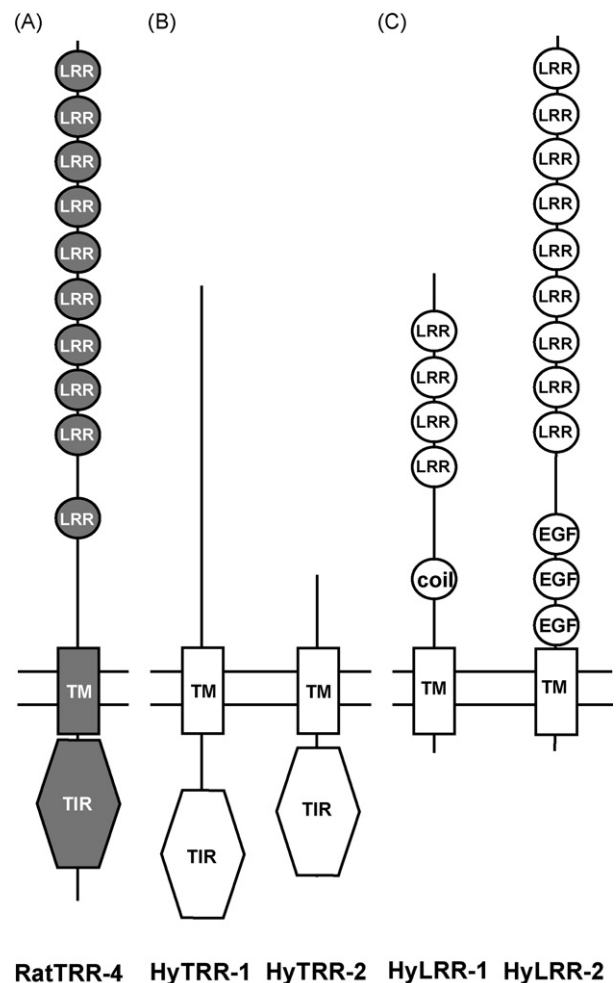


**Fig. 6.** Atypical putative TLR-like transmembrane receptors mediate the immune response in *Hydra*. (A) Rat TLR-4 showing the typical domain structure of TLRs with a cytoplasmic TIR domain and extracellular LRRs. (B) Domain structure of HyTRR-1 and HyTRR-2. (C) Domain structure of HyLRR-1 and HyLRR-2.

### 3.6. Atypical transmembrane receptors are involved in bacterial recognition in *Hydra*

In vertebrates, many of the PAMP-elicited signals including flagellin, LPS, and dsRNA are transduced by Toll-like receptors (TLRs) [3]. As reported previously [12], searching the available databases including the 170,000 *Hydra* ESTs (dbEST at NCBI) and the *H. magnipapillata* genomic sequences deposited at NCBI's Trace archive identified two genes whose inferred amino acid sequence contained a Toll/interleukin-1 receptor (TIR) domain, a transmembrane domain, and an extracellular domain lacking any specific domain structure (Fig. 6B). We have termed these *Hydra* genes Toll-receptor-related 1 (*HyTRR-1*) and Toll-receptor-related 2 (*HyTRR-2*) respectively (Fig. 6B). Most strikingly, neither *HyTRR-1* nor *HyTRR-2* contains leucine-rich repeats (LRRs) in its extracellular region (Fig. 6B). TBLASTN queries of the *H. magnipapillata* genome sequence and EST data set did not yield evidence for any additional *HyTRR-1* and *HyTRR-2* related genes [11,12]. The structures of *HyTRR-1* and *HyTRR-2* genes as well as predicted proteins are shown in Supplementary Figs. S2 and S3.

To study how these receptors function in the absence of LRRs, we screened the *Hydra* EST dataset as well as the *Hydra* genome for LRR-containing genes by using LRR sequences from human TLR4. We identified two full-length transcripts that encode putative transmembrane proteins carrying TLR-related LRRs on the extra-

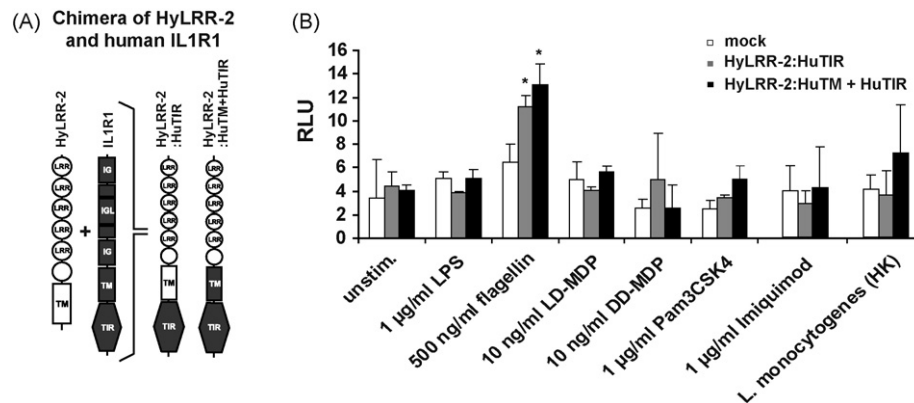


**Fig. 7.** HyLRR-2 mediates HEK293 cell activation by flagellin. (A) Schematic representation of chimeric proteins used illustrating the exchanged domains (grey). (B) NF-κB activation performed by transfection of HEK293 cells with chimeric HyLRR-2:HuTIR or HyLRR-2:HuTM + HuTIR.

cellular part (Fig. 6C). We termed these genes *HyLRR-1* and *HyLRR-2*, respectively. The two predicted LRR proteins contain up to eight LRR domains in their N-terminal region (Fig. 6C). Whereas *HyLRR-2* contains in addition three EGF domains, *HyLRR-1* has a coiled-coiled motif in the extracellular part. In both proteins, the transmembrane domain is followed by only a short stretch of amino acids near the C-terminal end with no obvious domain structure. The 2104 nucleotide containing full-length transcript of *HyLRR-2* shows a *Hydra* typical splice leader sequence (SL-B) at the 5' UTR and a poly A-tail at the 3' UTR. The structure of the complete *HyLRR-2* gene and gene product is shown in Supplementary Fig. S4.

3.7. *HyLRR-2* mediates HEK293 cell activation by flagellin

Since *HyLRR-2* is structurally more similar to vertebrate TLRs than *HyLRR-1*, we next examined whether this transmembrane protein can recognize PAMPs such as flagellin. To functionally assess the capacity of *HyLRR-2* to elicit intracellular signals induced by PAMP recognition, we generated several expression constructs encoding human/*Hydra* chimeric proteins (Fig. 7A). In a first set of experiments, the TIR domain of IL1R1, which is known to activate NF-κB via the recruitment of MyD88, was fused to the cytoplasmic region of *Hydra* *HyLRR-2* to generate an artificial, conventional TLR (*HyLRR-2:HuTIR*) (Fig. 7A). A second chimera combined the extracellular part of *HyLRR-2* to the transmembrane stalk and TIR domain of human IL1R1 (*HyLRR-2:HuTM + HuTIR*) (Fig. 7A). Using these chimeras, we next screened a library of PAMPs in order to determine the potential specificity of the chimeric receptor. For this purpose, HEK293 cells were transiently transfected with the two

plasmids and with a luciferase reporter construct driven by a 6× NF-κB consensus cassette. As shown in Fig. 7B, expression of the chimeric protein made HEK293 cells responsive to bacterial flagellin, demonstrating a functional flagellin receptor, whereas LPS or LD- or DD-MDP failed to activate HEK293 cells (Fig. 7B). Other PAMPs tested included PAM3CSK4, FSL-1, Poly(I:C), Imiquimod, ssRNA and CpG DNA, all of which did not result in a significant NF-κB activation with either of the plasmids (Fig. 7B).

3.8. Silencing of *HyLRR-2* affects expression of *HyTRR-1*

To investigate the role of the *HyLRR-2* receptor in antimicrobial effector molecule expression directly, we generated loss-of-function animals by dsRNA-mediated interference (RNAi). *HyLRR-2* dsRNA was synthesized and electroporated into intact polyps according to previously established protocols [19]. After 4 days, polyps showed distinct depletion of *HyLRR-2* transcripts (Fig. 8A, red box).

Unexpectedly, when examining the *HyLRR-2* loss-of function polyps we detected that also the level of *HyTRR-1* transcripts is markedly reduced (Fig. 8A). Since this observation raised the possibility that both transmembrane receptors, *HyLRR-2* and *HyTRR-1*, might influence each other, we next generated *HyTRR-1* loss-of function polyps and examined them for the level of *HyLRR-2* transcripts. As also shown in Fig. 8A, when *HyTRR-1* is knocked down by RNAi, the level of *HyLRR-2* transcripts is significantly reduced. Thus, *HyLRR-2* and *HyTRR-1* appear to have the specific ability to influence each other.

The *HyTRR-1* and *HyLRR-2* knockdowns did not have any notable effect on the survival of polyps (data not shown) but,

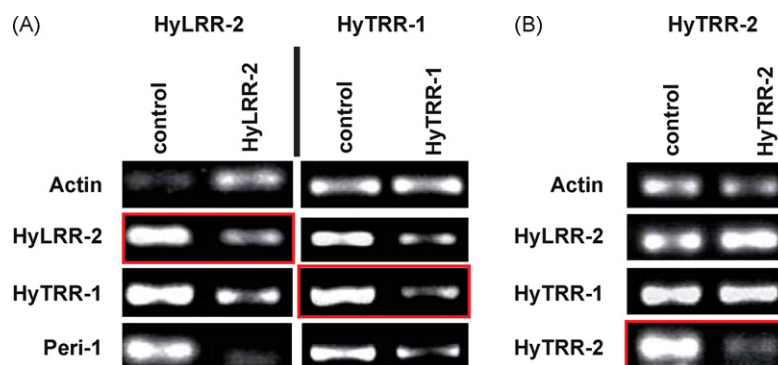


**Fig. 8.** Silencing of *HyLRR-2* affects expression of *HyTRR-1*. (A) Analysis of *HyTRR-1* and *HyLRR-2* loss-of-function polyps generated by RNAi. *HyTRR-1* loss-of-function polyps show a decreased expression of *HyLRR-2* and vice versa. In both RNAi experiments the transcription of the *Periculin-1* gene, coding for a novel bactericidal peptide, is also down regulated. (B) Control RNAi to demonstrate specificity of effects observed: *HyTRR-2* loss-of-function polyps generated by RNAi are affected in neither *HyLRR-2* nor *HyTRR-1* expression.

interestingly, resulted in a significant reduction of the level of *Periculin-1* expression (Fig. 8A) suggesting that the antimicrobial peptide encoding gene *Periculin-1* is downstream of the *HyLRR-2* mediated signalling cascade.

We next investigated whether the gene silencing effects shown in Fig. 8A reflected a specific interaction of both transmembrane proteins or whether any transmembrane receptor silencing would have similar effects. To test this and address the specificity of the RNAi effect described above, we generated loss-of-function polyps for the second TIR transmembrane receptor, *HyTRR-2*, and assessed them for expression of *HyTRR-1* and *HyLRR-2*. As shown in Fig. 8B, silencing of *HyTRR-2* expression failed to affect the level of *HyTRR-1* and *HyLRR-2* transcripts. Thus, *HyTRR-1* and *HyLRR-2* appear to interact with each other at the transcriptional level.

### 3.9. Flagellin-induced signalling requires direct interaction of both *HyLRR-2* and *HyTRR-1* proteins

To test our hypothesis that in *Hydra* recognition of flagellin is mediated by an intermolecular interaction of *HyLRR-2* as receptor

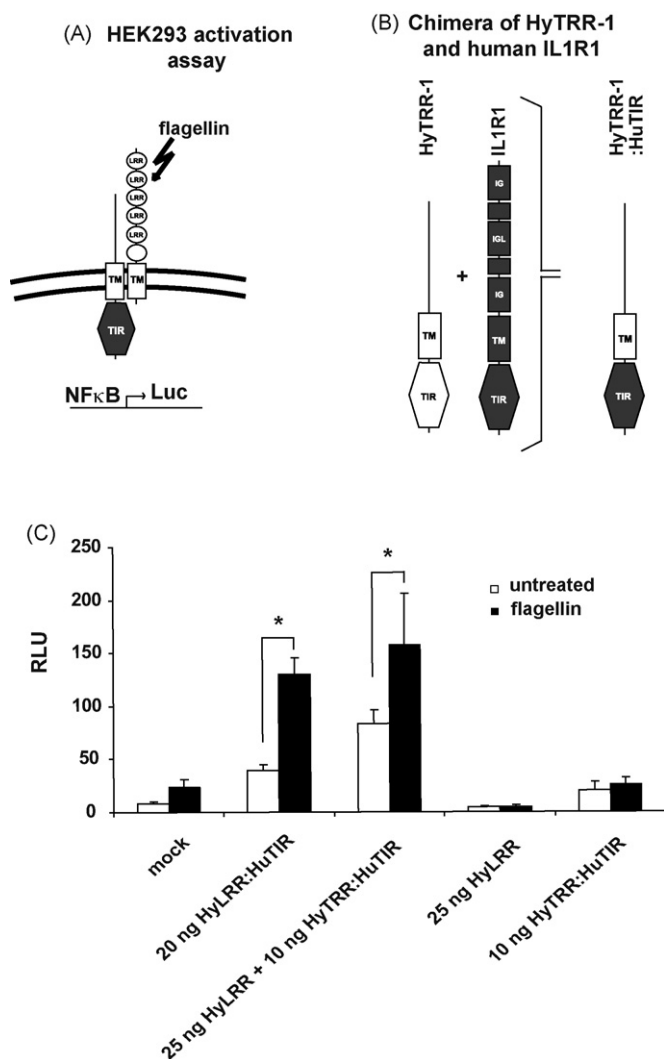


**Fig. 9.** Flagellin-induced signalling requires interaction of both *HyLRR-2* and *HyTRR-1* proteins. (A) Schematic representation of HEK293 activation assay. (B) Schematic representation of chimeric *HyTRR-1* protein used illustrating the exchanged domains (grey). (C) Only transfected cells expressing both transmembrane proteins, *HyTRR-1*:HuTIR and *HyLRR-2* showed an increased NF-κB activation induced by flagellin.

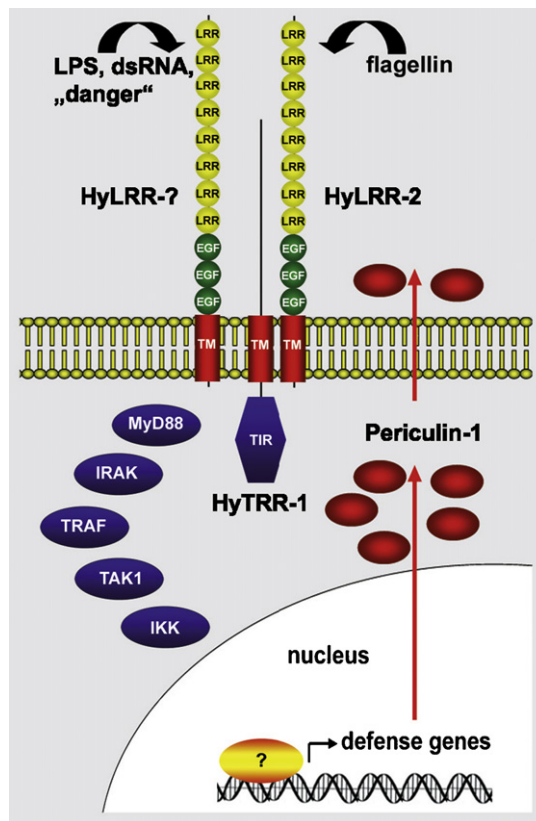


**Fig. 10.** Molecular components of the pathways involved in the *Hydra* epithelial host defence system. For details see text.

and *HyTRR-1* as signal transducer, we expressed the combination of *Hydra* *HyLRR-2* lacking the TIR domain together with *HyTRR-1* in human HEK293 cells (Fig. 9A). In order to elicit a signal in the ectopic expression system, the TIR domain of *HyTRR-1* was exchanged with the TIR domain of human IL1R1 (Fig. 9B). As shown in Fig. 9C, only transfected cells expressing both transmembrane proteins showed an increased NF-κB activation induced by flagellin. Cells transfected with *HyLRR-2* or *HyTRR-1* alone did not show an increase in NF-κB activation (Fig. 9C). These results support our view that in *Hydra* only the functional interaction of *Hydra* *HyLRR-2* and *HyTRR-1* mediates recognition of the bacterial PAMP flagellin. This receptor complex activation then is expected to trigger the innate immune response which involves the production of antimicrobial peptides (see Fig. 10 for model).

Most interestingly and supporting this view, in *HyTRR-1* silenced polyps we not only observed a significant reduction of *Periculin-1* expression (Fig. 8A) but also of the antimicrobial activity of tissue extract prepared from these animals. Using antimicrobial radial diffusion assays against *E. coli* we found that bacterial clearance was 29 mm<sup>2</sup> (S.D. ± 0.9, n = 6) when using tissue from RNAi polyps compared to 44 mm<sup>2</sup> (S.D. ± 4, n = 6) when using control tissue, which corresponds to a reduction of antimicrobial activity by about 34% in *HyTRR-1* loss-of-function polyps when compared to control polyps.

## 4. Discussion

The salient finding of this study is the identification of essential components mediating innate immunity in the freshwater polyp *Hydra*, which represents one of the phylogenetically oldest multicellular animals (see Fig. 1A). The results indicate that despite its morphological simplicity and the lack of

specialized phagocytes, *Hydra* has complex epithelial cell-based mechanisms for host defence and, therefore, is an attractive model for uncovering ancient innate defence strategies. The results enable us to propose a model (Fig. 10) in which direct recognition of PAMPs as well as indirect perception of pathological or toxicological processes within its tissue is mediated by atypical transmembrane receptors with the intracellular TIR domain and the extracellular LRRs being present on two different proteins. Following the activation of signal transduction pathways, epithelial cells mount an appropriate defence reaction. While previous searches in the *Hydra* database indicated [12] that signalling pathways may include conserved intracellular adapter proteins such as MyD88, IRAK, TRAF, TAK1 and IKK, here we provide experimental evidence that the *Hydra* host defence reaction is mediated by novel pathogen recognition receptors and engages novel potent antimicrobial peptides. We have previously shown [12] that *Nematostella*, an anthozoan Cnidaria, contains a classical TLR in which the intracellular TIR domain is connected to extracellular LRRs. A function of this receptor in innate immunity remains to be shown. However, since anthozoans phylogenetically are older than hydrozoans [11,12], the absence of a classical TLR in the *Hydra* genome implies that it was lost secondarily during evolution. This adds support to the view that the freshwater polyp *Hydra* – when compared to marine anthozoans – has accumulated a number of derived characters. Although our model (Fig. 10) describes a rather simplified view of an epithelial defence system, it captures an important feature: the *Hydra* epithelial defence system appears to employ both, evolutionary conserved signalling pathways as well as novel taxon-specific host defence-associated molecules. Thus, although the common ancestor of bilaterians appeared to recognize bacterial and tissue recognition molecules and activated an efficient epithelial defence system based on antimicrobial peptides, the precise nature of the pathogen-recognition system as well as details of the signalling pathways have been modified early during animal evolution and branched off into a variety of unique components in present day organisms.

#### 4.1. *Hydra*, an emerging model for the study of epithelial host defence mechanisms

Cnidaria share deep evolutionary connections with all animals including humans [45]. Our observation that antimicrobial host defence reactions in *Hydra* are solely mediated by epithelial cells as effector cells supports the recent hypothesis [10], that inducible expression of antimicrobial peptides in surface epithelia represents the ancestral system of host defence. More advanced invertebrates such as insects defend themselves against infection by a sophisticated set of reactions that involve blood cells, proteolytic cascades in the hemolymph, secretion of antimicrobial peptides from fat body cells as well as tissue-specific inducible expression of antimicrobial peptide genes in surface epithelia [46]. We note that ectodermal as well as endodermal epithelial cells in *Hydra* have previously been shown to be active phagocytes and are involved in tissue recognition and histocompatibility reactions [42,47]. This, together with the accessibility to comprehensive molecular biological analyses including transgenics [18], makes *Hydra* a valuable model to address certain aspects that are central to an understanding of the complexity of the innate immune system, but which are usually neglected in other models. These include the mechanisms protecting and maintaining epithelia in health and disease [48], the evolutionary relationship between innate immunity and regeneration [49], and between the innate immune system and the nervous system [50].

#### Acknowledgements

We thank S. Rathjen, M. Frank, and S. Hollmer for excellent technical contributions; U. Seydel and T. Gutschmann (Borstel) for LPS and LPS control; V. Klimovich and M. Samoilovich (St. Petersburg, Russia) for providing the anti-Periculin-1 antibody; all members of the Bosch lab for discussions; and J. Ittner-Bosch, K. Khalturin, J. Lohmann and D. Miller for helpful comments on the manuscript. The contributions of H. Stotz, H. Heine, and G. Genikhovich are acknowledged with gratitude. Sequencing of the SSH cDNA libraries was accomplished with support from the National Science Foundation (grants to HR Bode and RE Steele, UC Irvine, USA) and the Genome Sequencing Center in St. Louis. This work was supported by the Deutsche Forschungsgemeinschaft (SFB 617-A1; DFG 436 RUS 113/778) and the Clusters of Excellence “The Future Ocean” and “Inflammation at Interfaces”.

#### Appendix A. Supplementary data

Supplementary data associated with this article can be found, in the online version, at doi:10.1016/j.dci.2008.10.004.

#### References

- [1] Beutler B. Innate immunity: an overview. *Mol Immunol* 2004;40(12):845–59.
- [2] Medzhitov R, Janeway Jr CA. Decoding the patterns of self and nonself by the innate immune system. *Science* 2002;296(5566):298–300.
- [3] Akira S, Uematsu S, Takeuchi O. Pathogen recognition and innate immunity. *Cell* 2006;124(4):783–801.
- [4] Ferrandon D, Imler JL, Hetru C, Hoffmann JA. The *Drosophila* systemic immune response: sensing and signalling during bacterial and fungal infections. *Nat Rev Immunol* 2007;7(11):862–74.
- [5] Lemaitre B, Hoffmann J. The host defense of *Drosophila melanogaster*. *Annu Rev Immunol* 2007;25:697–743.
- [6] Wong D, Bazopoulou D, Pujol N, Tavernarakis N, Ewbank JJ. Genome-wide investigation reveals pathogen-specific and shared signatures in the response of *Caenorhabditis elegans* to infection. *Genome Biol* 2007;8(9):R194.
- [7] Alper S, McBride SJ, Lackford B, Freedman JH, Schwartz DA. Specificity and complexity of the *Caenorhabditis elegans* innate immune response. *Mol Cell Biol* 2007;27(15):5544–53.
- [8] Rast JP, Smith LC, Loza-Coll M, Hibino T, Litman GW. Genomic insights into the immune system of the sea urchin. *Science* 2006;314(5801):952–6.
- [9] Litman GW, Cannon JP, Dishaw LJ. Reconstructing immune phylogeny: new perspectives. *Nat Rev Immunol* 2005;5(11):866–79.
- [10] Ausubel FM. Are innate immune signaling pathways in plants and animals conserved? *Nat Immunol* 2005;6(10):973–9.
- [11] Hemmrich G, Miller DJ, Bosch TC. The evolution of immunity: a low-life perspective. *Trends Immunol* 2007;28(10):449–54.
- [12] Miller DJ, Hemmrich G, Ball EE, Hayward DC, Khalturin K, Funayama N, et al. The innate immune repertoire in cnidaria—ancestral complexity and stochastic gene loss. *Genome Biol* 2007;8(4):R59.
- [13] Fraune S, Bosch TCG. Long-term maintenance of species-specific bacterial microbiota in the basal metazoan *Hydra*. *Proc Natl Acad Sci USA* 2007;104(32):13146–51.
- [14] Bosch TCG. Why polyps regenerate and we don't: towards a cellular and molecular framework for *Hydra* regeneration. *Dev Biol* 2007;303(2):421–33.
- [15] Marcum BA, Fujisawa T, Sugiyama T. A mutant *hydra* strain (sf-1) containing temperature-sensitive interstitial cells. In: Tardent P, Tardent R, editors. *Developmental and cellular biology of coelenterates*. Elsevier: Amsterdam, North Holland; 1980. p. 429–34.
- [16] Kasahara S, Bosch TC. Enhanced antibacterial activity in *Hydra* polyps lacking nerve cells. *Dev Comp Immunol* 2003;27(2):79–85.
- [17] Cikala M, Wilms B, Hobmayer E, Bottger A, David CN. Identification of caspases and apoptosis in the simple metazoan *Hydra*. *Curr Biol* 1999;9(17):959–62.
- [18] Wittlieb J, Khalturin K, Lohmann JU, Anton-Erxleben F, Bosch TC. Transgenic *Hydra* allow in vivo tracking of individual stem cells during morphogenesis. *Proc Natl Acad Sci USA* 2006;103(16):6208–11.
- [19] Lohmann JU, Endl I, Bosch TC. Silencing of developmental genes in *Hydra*. *Dev Biol* 1999;214(1):211–4.
- [20] Lohmann JU, Bosch TC. The novel peptide HEADY specifies apical fate in a simple radially symmetric metazoan. *Genes Dev* 2000;14(21):2771–7.
- [21] Shi Y, Evans JE, Rock KL. Molecular identification of a danger signal that alerts the immune system to dying cells. *Nature* 2003;425(6957):516–21.
- [22] Sahly H, Schubert S, Harder J, Rautenberg P, Ullmann U, Schroder J, et al. Burkholderia is highly resistant to human Beta-defensin 3. *Antimicrob Agents Chemother* 2003;47(5):1739–41.

- [23] Genikhovich G, Kurn U, Hemmrich G, Bosch TC. Discovery of genes expressed in *Hydra* embryogenesis. *Dev Biol* 2006;289(2):466–81.
- [24] Diatchenko L, Lukyanov S, Lau YF, Siebert PD. Suppression subtractive hybridization: a versatile method for identifying differentially expressed genes. *Methods Enzymol* 1999;303:349–80.
- [25] Perteua G, Huang X, Liang F, Antonescu V, Sultana R, Karamycheva S, et al. TIGR Gene Indices clustering tools (TGICL): a software system for fast clustering of large EST datasets. *Bioinformatics* 2003;19(5):651–2.
- [26] Altschul SF, Gish W, Miller W, Myers EW, Lipman DJ. Basic local alignment search tool. *J Mol Biol* 1990;215(3):403–10.
- [27] Chenna R, Sugawara H, Koike T, Lopez R, Gibson TJ, Higgins DG, et al. Multiple sequence alignment with the Clustal series of programs. *Nucleic Acids Res* 2003;31(13):3497–500.
- [28] Kumar S, Tamura K, Nei M. MEGA3: integrated software for molecular evolutionary genetics analysis and sequence alignment. *Brief Bioinform* 2004;5(2):150–63.
- [29] Letunic I, Copley RR, Schmidt S, Ciccarelli FD, Doerks T, Schultz J, et al. SMART 4.0: towards genomic data integration. *Nucleic Acids Res* 2004;32(Database issue):D142–144.
- [30] Bendtsen JD, Nielsen H, von Heijne G, Brunak S. Improved prediction of signal peptides: SignalP 3.0. *J Mol Biol* 2004;340(4):783–95.
- [31] Eddy SR. Profile hidden Markov models. *Bioinformatics* 1998;14(9):755–63.
- [32] Glaser R, Harder J, Lange H, Bartels J, Christophers E, Schroder JM. Antimicrobial psoriasin (S100A7) protects human skin from *Escherichia coli* infection. *Nat Immunol* 2005;6(1):57–64.
- [33] Harder J, Bartels J, Christophers E, Schroder JM. Isolation and characterization of human beta-defensin-3, a novel human inducible peptide antibiotic. *J Biol Chem* 2001;276(8):5707–13.
- [34] Harder J, Schroder JM. RNase 7, a novel innate immune defense antimicrobial protein of healthy human skin. *J Biol Chem* 2002;277(48):46779–84.
- [35] Schroder JM. Identification and structural characterization of chemokines in lesional skin material of patients with inflammatory skin disease. *Methods Enzymol* 1997;288:266–97.
- [36] Zasloff M. Antimicrobial peptides of multicellular organisms. *Nature* 2002;415(6870):389–95.
- [37] Tasiemski A, Vandenbulcke F, Mitta G, Lemoine J, Lefebvre C, Sautiere PE, et al. Molecular characterization of two novel antibacterial peptides inducible upon bacterial challenge in an annelid, the leech *Theromyzon tessulatum*. *J Biol Chem* 2004;279(30):30973–82.
- [38] Seydel U, Schromm AB, Brade L, Gronow S, Andra J, Muller M, et al. Physico-chemical characterization of carboxymethyl lipid A derivatives in relation to biological activity. *Febs J* 2005;272(2):327–40.
- [39] Ashburner M, Ball CA, Blake JA, Botstein D, Butler H, Cherry JM, et al. Gene ontology: tool for the unification of biology. The Gene Ontology Consortium. *Nat Genet* 2000;25(1):25–9.
- [40] Johnson CL, Gale Jr M. CARD games between virus and host get a new player. *Trends Immunol* 2006;27(1):1–4.
- [41] Kuznetsov S, Lyanguzowa M, Bosch TC. Role of epithelial cells and programmed cell death in *Hydra* spermatogenesis. *Zoology (Jena)* 2001;104(1):25–31.
- [42] Bosch TCG, David CN. Growth regulation in *Hydra*: relationship between epithelial cell cycle length and growth rate. *Dev Biol* 1984;104(1):161–71.
- [43] Martinon F, Petrilli V, Mayor A, Tardivel A, Tschopp J. Gout-associated uric acid crystals activate the NALP3 inflammasome. *Nature* 2006;440(7081):237–41.
- [44] Matzinger P. The danger model: a renewed sense of self. *Science* 2002;296(5566):301–5.
- [45] Technau U, Rudd S, Maxwell P, Gordon PM, Saina M, Grasso LC, et al. Maintenance of ancestral complexity and non-metazoan genes in two basal cnidarians. *Trends Genet* 2005;21(12):633–9.
- [46] Khush RS, Leulier F, Lemaitre B. Immunology. Pathogen surveillance—the flies have it. *Science* 2002;296(5566):273–5.
- [47] Bosch TCG, David DC. Immunocompetence in *Hydra*: epithelial cells recognize self-nonsel and react against it. *J Exp Zool* 1986;238:225–34.
- [48] Schreiber S, Rosenstiel P, Albrecht M, Hampe J, Krawczak M. Genetics of Crohn disease, an archetypal inflammatory barrier disease. *Nat Rev Genet* 2005;6(5):376–88.
- [49] Harty M, Neff AW, King MW, Mescher AL. Regeneration or scarring: an immunologic perspective. *Dev Dyn* 2003;226(2):268–79.
- [50] Brogden KA, Guthmiller JM, Salzet M, Zasloff M. The nervous system and innate immunity: the neuropeptide connection. *Nat Immunol* 2005;6(6):558–64.